

4. L. M. Mack, "Boundary-layer stability theory, Part 2," Jet Propulsion Lab. Doc, No. 900-277 (Rev. A), Pasadena, CA (1969).
5. V. R. Gushchin and A. V. Fedorov, "Excitation and development of unstable disturbances in a supersonic boundary layer," *Izv. Akad. Nauk SSSR, Mekh. Zhidk. Gaza*, No. 3 (1990).
6. V. R. Gushchin and A. V. Fedorov, "Qualitative characteristics of the instability of flows near a wall at large flow velocities," in: *Models of the Mechanics of Inhomogeneous Systems [in Russian]*, ITPM SO AN SSSR, Novosibirsk (1989).
7. G. V. Petrov, "Two-dimensional absolute instability of a supersonic boundary layer," *Izv. Akad. Nauk SSSR, Mekh. Zhidk. Gaza*, No. 1 (1988).
8. G. V. Petrov, "Stability of thin shock layer on wedge in hypersonic flow of a perfect gas," in: *Laminar-Turbulent Transition: IUTAM Symposium*, Novosibirsk (1984).
9. V. R. Gushchin and A. V. Fedorov, "Short-wave instability in a shock layer of an ideal gas," *Izv. Akad. Nauk SSSR, Mekh. Zhidk. Gaza*, No. 1 (1989).
10. A. H. Nayfeh, "Stability of three-dimensional boundary layers," *AIAA J.*, 18, No. 4 (1980).
11. S. A. Lomov, *Introduction to the General Theory of Singular Perturbations [in Russian]*, Nauka, Moscow (1981).
12. M. V. Fedoryuk, *Asymptotic Methods for Linear Ordinary Differential Equations [in Russian]*, Nauka, Moscow (1983).

TURBULENT FLOW OF A GAS SUSPENSATE WHOSE PARTICLES
INTERACT STRONGLY WITH THE CHANNEL WALLS

I. V. Derevich

UDC 532.529

Turbulent two-phase gas flows are widely used in power engineering, aviation, and chemical engineering. In the pneumatic transport of a powder, one frequently has fairly coarse particles, whose dynamic relaxation times may greatly exceed the characteristic time scale of the turbulent pulsations. In that case, the pulsating and average motion of the powder is substantially different from that for small particles, whose dynamic relaxation times are less than or comparable with the time scale of the velocity pulsations in the liquid phase. The extent of the pulsating motion for small particles is determined by the extent to which the powder is extrained in the turbulent motion and can be estimated in the local-equilibrium approximation without considering the collisions of the particles with the channel walls [1]. The average and pulsating characteristics for large particles are dependent on the interaction with the walls. There are effects from the marked velocity difference between the phases and the intense chaotic motion of the powder, where the level of the pulsating motion for the powder may greatly exceed that of the particle pulsation in an unbounded space with identical turbulence intensity, and this can be explained only on the basis of the collisions between inertial particles and the bounding surfaces. The collisions cause the particles to lose momentum and to rotate around the points of contact. The Magnus force arising from the rotation causes rapid transverse displacement [2, 3]. The channel walls in a gas-power system thus provide positive feedback, which causes additional pulsations in the powder by comparison with turbulent flow in an unbounded space.

There are two approaches to calculating the characteristics of such flows. Firstly, there is direct stochastic simulation, which is based on solving the equations of motion for a single particle in a random velocity pattern [2, 5-8]. However, to obtain information on the averaged characteristics, it is necessary to calculate many thousands of such paths, which consumes considerable time. In spite of the apparent simplicity, the method of calculating Lagrange paths is not widely used in designing pneumatic transport systems. The second method is based on the conservation equations for mass, momentum, and angular momentum of the particles and the intensity of the turbulent pulsations [3, 9]. Then to close the system, it is necessary to derive expressions representing the rate of turbulent momentum transport, the angular momentum, and the pulsation energy, and also to substitute boundary conditions for the equations for the first and second moments, which incorporate the inter-

Moscow. Translated from *Prikladnaya Mekhanika i Tekhnicheskaya Fizika*, No. 6, pp. 73-81, November-December, 1992. Original article submitted November 25, 1991.

action with the walls. Formulas have been derived for the turbulent energy transport by the powder in a particular case from the equations for the corresponding third moments, with subsequent use of Millionshchikov's hypothesis on the fourth moments [10]. It is no simple task to formulate the boundary conditions for the conservation equations for the powder. In [9, 11], boundary conditions have been derived for the conservation equations for mass, momentum, and the second moments of the particle velocity pulsations subject to the condition that the particles lose part of their momentum by collision with the wall. The boundary conditions in [3] have been written on the assumption of δ distributions for the velocities and angular velocities of the particles incident on the wall, with the boundary conditions containing the velocity ratio for the rotation before and after collision, which requires additional empirical information on the rotational velocities.

Here is derived a closed equation for the probability density PD in terms of the coordinates, velocities, and angular velocities of the particles; an equation system is written for the first and second moments of the velocity and angular velocity pulsations. An approximate solution is obtained to the kinetic equation that incorporates terms linear in the gradients of the powder characteristics and expressions are derived representing the turbulent transport of momentum, angular momentum, and the turbulent powder velocity pulsations. Boundary conditions are derived for the conservation equations for mass, momentum, angular momentum, and pulsation energy, which incorporate the momentum loss and the rapid rotation resulting from collision. Calculations are performed on the powder characteristics in horizontal and vertical channels for rising and descending suspensate flows.

1. PD Equation and Equation System for the First and Second Moments. We consider the flow of a gas suspensate without back reaction from the powder on the characteristics of the carrying flow, which corresponds to a flow in which the weight concentration of the particles is much less than one. We take the characteristics of the fluid phase as known and consider the PD for the particles averaged over realizations of the turbulent flow:

$$\langle \Phi(\mathbf{x}, \mathbf{V}, \boldsymbol{\Omega}, t) \rangle = \langle \delta(\mathbf{x} - \mathbf{R}_p) \delta(\mathbf{V} - \mathbf{V}_p) \delta(\boldsymbol{\Omega} - \boldsymbol{\Omega}_p) \rangle.$$

Here the following are the equations of motion for a single particle, which describe the coordinate \mathbf{R}_p , the velocity \mathbf{V}_p , and the angular velocity $\boldsymbol{\Omega}_p$ [1-3]:

$$\begin{aligned} \frac{dR_{pi}}{dt} &= V_{pi}(t), \\ \frac{dV_{pi}}{dt} &= \frac{1}{\tau} (U_i(\mathbf{R}_p, t) + \tau g_i - V_{pi}) - \gamma_\omega \varepsilon_{ijk} \Omega_{pk} (U_j(\mathbf{R}_p, t) - V_{pj}), \\ \frac{d\Omega_{pi}}{dt} &= -\frac{1}{\tau_\omega} \Omega_{pi}(t), \end{aligned} \quad (1.1)$$

in which τ and τ_ω are the dynamic relaxation times for the velocity and angular velocity, ε_{ijk} is an antisymmetric tensor, $U_i(\mathbf{x}, t) = \langle U_i(\mathbf{x}, t) \rangle + u_i(\mathbf{x}, t)$ being the velocity of the carrying phase, in which the averaged and pulsating components are distinguished, and the value of the constant γ_ω is dependent on the velocity of the flow around the particles and is proportional to the ratio of the densities of the gas and the particle material, $\gamma_\omega \sim \rho_g / \rho_p$, while g_i is the acceleration due to gravity.

For inertial particles, $\tau \gg T_E$ (T_E is the characteristic time scale of the turbulent pulsations for the fluid phase), and the velocity pulsations in the carrying phase can be represented as a Gaussian random field δ -correlated in time:

$$\langle u_i(\mathbf{x}_1, t) u_j(\mathbf{x}_2, t + s) \rangle = T_E \langle u_i(\mathbf{x}_1, t) u_j(\mathbf{x}_2, t) \rangle \delta(s).$$

Functional differentiation [12] gives us by analogy with [9] a closed equation for the particle PD:

$$\begin{aligned} \frac{D\langle \Phi \rangle}{Dt} + \left\{ -\frac{D\langle V_k \rangle}{Dt} + \frac{\langle U_k \rangle + \tau g_k - \langle V_k \rangle}{\tau} - \gamma_\omega \varepsilon_{ijk} \langle \Omega_i \rangle (\langle U_j \rangle - \langle V_j \rangle) - \langle \Omega_j \rangle v_j + \omega_i (\langle U_j \rangle - \langle V_j \rangle) - \omega_i v_j \right\} \frac{\partial \langle \Phi \rangle}{\partial v_k} - \left(\frac{D\langle \Omega_k \rangle}{Dt} + \frac{\langle \Omega_k \rangle}{\tau_\omega} \right) \frac{\partial \langle \Phi \rangle}{\partial \omega_k} - \\ - v_k \frac{\partial \langle V_i \rangle}{\partial x_k} \frac{\partial \langle \Phi \rangle}{\partial v_i} - v_k \frac{\partial \langle \Omega_i \rangle}{\partial x_k} \frac{\partial \langle \Phi \rangle}{\partial \omega_i} - \frac{1}{\tau} \frac{\partial}{\partial v_k} \langle \Phi \rangle - \frac{1}{\tau_\omega} \frac{\partial}{\partial \omega_k} \omega_k \langle \Phi \rangle = \end{aligned} \quad (1.2)$$

$$\begin{aligned}
&= \left[\frac{T_E}{\tau} \langle u_j u_k \rangle - \frac{2T_E}{\tau} \gamma_{\omega} \varepsilon_{ink} (\langle \Omega_i \rangle + \omega_i) \langle u_j u_n \rangle + T_E \gamma_{\omega}^2 \varepsilon_{nlj} \varepsilon_{imk} \langle u_m u_l \rangle \times \right. \\
&\quad \left. \times (\langle \Omega_n \rangle + \omega_n) (\langle \Omega_i \rangle + \omega_i) \right] \frac{\partial^2 \langle \Phi \rangle}{\partial v_j \partial v_k}, \\
\frac{D}{Dt} &= \frac{\partial}{\partial t} + \langle V_k \rangle \frac{\partial}{\partial x_k}, \quad v_i = V_i - \langle V_i \rangle, \quad \omega_i = \Omega_i - \langle \Omega_i \rangle, \\
\langle V_i \rangle \langle N \rangle &= \int dV \int d\Omega V_i \langle \Phi \rangle, \quad \langle \Omega_i \rangle \langle N \rangle = \int dV \int d\Omega \Omega_i \langle \Phi \rangle, \\
\langle N \rangle &= \int dV \int d\Omega \langle \Phi \rangle
\end{aligned}$$

$\langle N \rangle$, $\langle V_i \rangle$, $\langle \Omega_i \rangle$ are the averaged number concentration of the particles, velocity, and angular velocity. Equation (1.2) is the Fokker-Planck equation extended to the case of rotating particles. From (1.2) we get a system for the first and second moments of the pulsations in the velocity and angular velocity:

$$\begin{aligned}
&\frac{\partial \langle N \rangle}{\partial t} + \frac{\partial}{\partial x_k} \langle N \rangle \langle V_k \rangle = 0, \\
\frac{D \langle V_i \rangle}{Dt} + \frac{1}{\langle N \rangle} \frac{\partial \langle N \rangle \langle v_i v_k \rangle}{\partial x_k} &= \frac{\langle U_i \rangle + \tau g_i - \langle V_i \rangle}{\tau} - \\
&- \gamma_{\omega} \varepsilon_{ijk} (\langle \Omega_k \rangle (\langle U_j \rangle - \langle V_j \rangle) - \langle \omega_k v_j \rangle), \\
\frac{D \langle \Omega_i \rangle}{Dt} + \frac{1}{\langle N \rangle} \frac{\partial \langle N \rangle \langle \omega_i v_k \rangle}{\partial x_k} &= - \frac{\langle \Omega_i \rangle}{\tau_{\omega}}, \\
\frac{D \langle v_i v_j \rangle}{Dt} + \frac{1}{\langle N \rangle} \frac{\partial \langle N \rangle \langle v_i v_j v_k \rangle}{\partial x_k} + \langle v_i v_k \rangle \frac{\partial \langle V_j \rangle}{\partial x_k} + \langle v_j v_k \rangle \frac{\partial \langle V_i \rangle}{\partial x_k} &= \frac{2}{\tau} (\sigma_{ij}^0 - \langle v_i v_j \rangle), \\
\sigma_{ij}^0 &= \frac{T_E}{\tau} \langle u_i u_j \rangle - \frac{\tau \gamma_{\omega}}{2} \left\{ \varepsilon_{lmj} [(\langle U_m \rangle - \langle V_m \rangle) \langle \omega_l v_i \rangle + \langle \Omega_l \rangle \left(\frac{T_E}{\tau} \langle u_m u_i \rangle - \right. \right. \\
&- \langle v_m v_i \rangle) - \langle \omega_l v_m v_i \rangle] + \varepsilon_{lmi} [(\langle U_m \rangle - \langle V_m \rangle) \langle \omega_l v_j \rangle + \langle \Omega_l \rangle \left(\frac{T_E}{\tau} \langle u_m u_j \rangle - \right. \\
&- \langle v_m v_j \rangle) - \langle \omega_l v_m v_j \rangle] \left. \right\} + \frac{T_E \tau \gamma_{\omega}^2}{2} \varepsilon_{nlj} \varepsilon_{kmi} \langle u_m u_l \rangle (\langle \Omega_n \rangle \langle \Omega_k \rangle + \langle \omega_n \omega_k \rangle), \\
\frac{D \langle \omega_i \omega_j \rangle}{Dt} + \frac{1}{\langle N \rangle} \frac{\partial \langle N \rangle \langle \omega_i \omega_j v_k \rangle}{\partial x_k} + \langle \omega_i v_k \rangle \frac{\partial \langle \Omega_j \rangle}{\partial x_k} + \langle \omega_j v_k \rangle \frac{\partial \langle \Omega_i \rangle}{\partial x_k} &= - \frac{2}{\tau_{\omega}} \langle \omega_i \omega_j \rangle, \\
\frac{D \langle \omega_i v_j \rangle}{Dt} + \frac{1}{\langle N \rangle} \frac{\partial \langle N \rangle \langle \omega_i v_j v_k \rangle}{\partial x_k} + \langle \omega_i v_k \rangle \frac{\partial \langle V_j \rangle}{\partial x_k} + \langle v_j v_k \rangle \frac{\partial \langle \Omega_i \rangle}{\partial x_k} + \\
&+ \gamma_{\omega} \varepsilon_{lmj} [\langle \omega_l \omega_i \rangle (\langle U_m \rangle - \langle V_m \rangle) - \langle \Omega_l \rangle \langle v_m \omega_i \rangle - \langle \omega_l \omega_i v_m \rangle] = \\
&= - \left(\frac{1}{\tau} + \frac{1}{\tau_{\omega}} \right)^{-1} \langle \omega_i v_j \rangle.
\end{aligned}$$

Here the second moments of the pulsations in the velocity and angular velocity of the particles $\langle v_i v_j \rangle$, $\langle v_i \omega_j \rangle$ are turbulent fluxes of momentum and angular momentum arising as a result of the pulsating motion of the powder. The third moments of the pulsations $\langle v_i v_j v_k \rangle$, $\langle \omega_i \omega_j v_k \rangle$, $\langle \omega_i v_j v_k \rangle$ represent turbulent transport of the intensity of the random particle motion.

To close the system and construct the boundary conditions, an approximate method of solving (1.2) is used. The averaged characteristics for the powder vary little over the cross section. When one solves the kinetic equation, one can restrict oneself to terms linear in the gradients of the averaged parameters for the powder. From (1.1) and (1.2) we have that rotation arises only by collision with the channel wall. The zeroth approximation in the solution to the kinetic equation is

$$\begin{aligned}
\langle \Phi_0(\mathbf{x}, \mathbf{v}, \boldsymbol{\omega}, t) \rangle &= \langle N \rangle \varphi_0(\mathbf{v}) \delta(\boldsymbol{\omega}), \\
\varphi_0(\mathbf{v}) &= \prod_{i=1}^3 (2\pi\sigma_{ii})^{-1/2} \exp\left(-\frac{v_i v_i}{2\sigma_{ii}}\right), \quad \sigma_{ii} = \langle v_i v_i \rangle.
\end{aligned}$$

We close the system for the first and second moments in the zeroth approximation and apply a procedure to solve (1.2) analogous to the Chapman-Enskog method [13], which gives an approxi-

mate solution for the PD linear in the gradients of the averaged powder parameters:

$$\begin{aligned} \langle \Phi(\mathbf{x}, \mathbf{v}, \omega, t) \rangle = \langle N \rangle \varphi_0 \left\{ 1 + \frac{1}{2} \sigma_{ih}^0 (1 - \delta_{ih}) \frac{v_i v_h}{\sigma_{ii} \sigma_{hh}} - \frac{\tau}{2\sigma_{ii}} (v_i v_h - \right. \\ \left. - \delta_{ih} v^2) \frac{\partial \langle V_i \rangle}{\partial x_h} - \frac{\tau}{3} v_h \left[\frac{v_i^2}{2\delta_{ii}} - \left(\frac{1}{2} + \delta_{ih} \right) \right] \frac{\partial \ln \sigma_{ii}}{\partial x_h} \right\} \delta(\omega) + \\ + \langle N \rangle \varphi_0 \left(\frac{1}{\tau} + \frac{1}{\tau_\omega} \right)^{-1} v_h \frac{\partial \langle \Omega_i \rangle}{\partial x_h} \frac{\partial \delta(\omega)}{\partial \omega_i}. \end{aligned} \quad (1.3)$$

This enables one to calculate expressions for the second and third moments of the velocity and angular velocity pulsations:

$$\begin{aligned} \langle v_i v_j \rangle = \sigma_{ii} \delta_{ij} + (1 - \delta_{ij}) \sigma_{ij}^0 - \frac{\tau}{2} \left[\sigma_{ii} \frac{\partial \langle V_j \rangle}{\partial x_i} + \sigma_{jj} \frac{\partial \langle V_i \rangle}{\partial x_j} - \frac{2}{3} \delta_{ij} \sigma_{hh} \frac{\partial \langle V_h \rangle}{\partial x_k} \right], \\ \langle v_i \omega_j \rangle = - \left(\frac{1}{\tau} + \frac{1}{\tau_\omega} \right)^{-1} \langle v_i v_h \rangle \frac{\partial \langle \Omega_j \rangle}{\partial x_h}, \quad \langle \omega_i \omega_j \rangle = 0, \\ \langle v_i \omega_j \omega_k \rangle = 0, \quad \langle v_i v_j v_h \rangle = - \delta_{ij} \frac{2\delta_{ih} + \delta_{ii}}{3} \tau \sigma_{hh} \frac{\partial \sigma_{ii}}{\partial x_h}, \\ \langle \omega_l v_m v_j \rangle = - \left(\frac{1}{\tau} + \frac{1}{\tau_\omega} \right)^{-1} \langle v_h v_m v_j \rangle \frac{\partial \langle \Omega_l \rangle}{\partial x_h}. \end{aligned}$$

2. Boundary Conditions. We consider a model for the collision with the surface in which the momenta of particles reflected along the y and z axes constitute k_n and k_t , when the parts of the momenta of the incident particles (the y axis is normal to the surface and the x axis coincides with the flow direction, while the direction of a reflected particle's momentum along the y axis is opposite to the direction of that for an incident one), while the axial velocities and rotational velocities of the incident and reflected particles are [1-3] related by

$$\begin{aligned} V_x'' = \alpha_1 V_x' + \alpha_2 \Omega_z', \quad \Omega_z'' = \beta_1 V_x' + \beta_2 \Omega_z', \quad V_y'' = -k_n V_y', \quad V_z'' = k_t V_z', \\ \alpha_1 = \frac{5 + 2k_t}{7}, \quad \alpha_2 = -d_p \frac{1 - k_t}{7}, \quad \beta_1 = -\frac{10(1 - k_t)}{7 d_p}, \quad \beta_2 = \frac{5k_t + 2}{7} \end{aligned} \quad (2.1)$$

(a prime denotes a quantity before collision with the wall, and two primes denotes one after collision).

The PD for reflected particles is related to that for the incident ones by

$$\begin{aligned} \langle \Phi_+(x, \mathbf{V}'', \boldsymbol{\Omega}'', t) \rangle = \int_{-\infty}^{\infty} dV_x' \int_{-\infty}^0 dV_y' \int_{-\infty}^{\infty} dV_z' \int_{-\infty}^{\infty} d\Omega_z' G(\mathbf{V}'', \boldsymbol{\Omega}''; \mathbf{V}', \boldsymbol{\Omega}') \times \\ \times \langle \Phi(x, \mathbf{V}', \boldsymbol{\Omega}', t) \rangle, \quad V_y'' > 0, \end{aligned}$$

where the kernel is explicitly dependent on (2.1), which describes the result of collision with the surface:

$$\begin{aligned} G(\mathbf{V}'', \boldsymbol{\Omega}''; \mathbf{V}', \boldsymbol{\Omega}') = \delta(V_z'' - k_t V_z') \delta(V_y'' + k_n V_y') \delta(\beta_2 V_x'' - \alpha_2 \Omega_z'' - k_t V_z') \times \\ \times \delta(\alpha_1 \Omega_z'' - \beta_1 V_x'' - k_t \Omega_z'). \end{aligned}$$

We calculate the sum of the fluxes of the powder for the incident and reflected particles and equate this to the flux in the flow as referred to the surface [9, 11] to get the boundary conditions for the normal and axial velocities of the powder, the angular velocity, and the intensities of the transverse and longitudinal particle velocity pulsations ($y = 0$):

$$\begin{aligned} \langle V_y \rangle + \frac{1 - k_n}{1 + k_n} \left(\frac{2}{\pi} \sigma_{yy} \right)^{1/2} = 0, \\ \frac{\tau \sigma_{yy}}{2} \frac{\partial \langle V_x \rangle}{\partial y} - \left[\langle V_y \rangle + \left(\frac{2}{\pi} \sigma_{yy} \right)^{1/2} \frac{1 - k_n^2 k_t - (3/7) k_n (1 - k_t)}{1 + k_n (1 + k_t) + k_n^2 k_t} \right] \langle V_x \rangle = \end{aligned}$$

$$\begin{aligned}
&= -\frac{2k_n\alpha_2}{1+k_n(1+k_t)+k_n^2k_t} \left(\frac{2}{\pi}\sigma_{yy}\right)^{1/2} \langle\Omega_z\rangle, \\
\left(\frac{1}{\tau} + \frac{1}{\tau_\omega}\right)^{-1} \sigma_{yy} \frac{\partial\langle\Omega_z\rangle}{\partial y} - \left[\langle V_y\rangle + \left(\frac{2}{\pi}\sigma_{yy}\right)^{1/2} \frac{1-k_n^2k_t+(3/7)k_n(1-k_t)}{1+k_n(1+k_t)+k_n^2k_t}\right] \langle\Omega_z\rangle &= \\
&= -\frac{2k_n\beta_1}{1+k_n(1+k_t)+k_n^2k_t} \left(\frac{2}{\pi}\sigma_{yy}\right)^{1/2} \langle V_x\rangle, \\
\tau\sigma_{yy} \frac{\partial\sigma_{yy}}{\partial y} - \left[\langle V_y\rangle + 2\left(\frac{2}{\pi}\sigma_{yy}\right)^{1/2} \frac{1-k_n^3}{1+k_n^3}\right] \sigma_{yy} &= 0, \\
\frac{\tau}{3}\sigma_{yy} \frac{\partial\sigma_{xx}}{\partial y} - \left[\langle V_y\rangle + \left(\frac{2}{\pi}\sigma_{yy}\right)^{1/2} \frac{1-k_n\alpha_1^2}{1+k_n\alpha_1^2}\right] \sigma_{xx} &= 0.
\end{aligned}$$

These boundary conditions extend those derived in [9, 11] for the flow of particles in rotation resulting from collision with the wall.

3. Results. The calculations were performed for the stabilized part of the flow in a circular tube. A cylindrical coordinate system (r, θ, z) was used, where the conservation equations for the momentum, angular momentum, and particle concentration in dimensionless variables are

$$\begin{aligned}
&\frac{1}{(1-\bar{y})\bar{N}} \frac{d}{d\bar{y}} \left[(1-\bar{y})\bar{N} \frac{\tau^+\sigma_{yy}^+ d\bar{V}_x}{2 d\bar{y}} \right] - V_y^+ \frac{d\bar{V}_x}{d\bar{y}} R^+ - \\
&\quad - \frac{R^{+2}}{\tau^+} \bar{V}_x = -\frac{R^{+2}}{\tau^+} \bar{U}'_x, \\
\bar{U}'_x = \bar{U}_x - \gamma_\omega \left[\bar{\Omega} (U_y^+ - V_y^+) \frac{St}{U_m^+} + \left(1 + \frac{\tau}{\tau_\omega}\right)^{-1} \frac{St^2}{U_m^+} \sigma_{yy} \frac{d\bar{\Omega}}{d\bar{y}} \right] + St \bar{g}_x, \\
&\frac{1}{(1-\bar{y})\bar{N}} \frac{d}{d\bar{y}} \left[(1-\bar{y})\bar{N}\tau^+ \left(1 + \frac{\tau}{\tau_\omega}\right)^{-1} \sigma_{yy}^+ \frac{d\bar{\Omega}}{d\bar{y}} \right] - R^+ V_y^+ \frac{d\bar{\Omega}}{d\bar{y}} - \\
&\quad - \frac{R^{+2}}{\tau^+} \left(\frac{\tau}{\tau_\omega}\right) \bar{\Omega} = 0, \\
\tau^+\sigma_{yy}^+ \frac{d\bar{N}}{d\bar{y}} - R^+ (V_{mig}^+ + \bar{U}_y^+) \bar{N} = R^+ (1-\bar{y}) J^+ = -\bar{N} V_y^+, \\
J^+ = \left(\frac{2}{\pi}\sigma_{yy}^+\right)^{1/2} \frac{1-k_n}{1+k_n} \bar{N}_w, N_m = 2 \int_0^1 d\bar{y} (1-\bar{y}) \langle N \rangle, \\
\bar{N} = \langle N \rangle / N_m, V_{mig}^+ = \frac{\tau^+}{R^+} \frac{d\sigma_{yy}^+}{d\bar{y}}, \\
\bar{U}_y^+ = \gamma_\omega \left[St U_m^+ \bar{\Omega} (\bar{U}_x - \bar{V}_x) - \left(1 + \frac{\tau}{\tau_\omega}\right)^{-1} \frac{St^3}{2U_m^+} \sigma_{yy}^+ \frac{d\bar{\Omega}}{d\bar{y}} \frac{d\bar{V}_x}{d\bar{y}} \right] + U_y^+,
\end{aligned} \tag{3.1}$$

in which $\bar{U} = \langle U \rangle / U_m$; $\bar{V} = \langle V \rangle / U_m$ (U_m is the mean mass velocity), $U_m^+ = U_m / u_+$ (u_+ is the dynamic velocity of the fluid phase), $R^+ = Ru^+ / \nu$ (R channel radius), ν the kinematic viscosity of the gas, $\tau^+ = \tau u_+^2 / \nu$; $St = \tau U_m / R$ the Stokes number for the particles, $\bar{\Omega} = \Omega_\theta R / U_m$ the dimensionless rotational velocity, V_{mig} the velocity of the turbulent particle migration caused by inhomogeneity in the pulsation energy for the powder phase, $J^+ = J / u_+$ the particle flux at the channel wall, \bar{N}_w the concentration of the powder at the surface, $\bar{y} = 1 - r/R$; r the radial coordinate, and $\bar{g}_x = g_x R / U_m^2$.

The boundary conditions for (3.1) reflect the flow symmetry at the axis, the lack of rotation in the flow of powder at the axis, and the particle rotation arising from collision with the wall:

$$\begin{aligned}
\bar{y} = 1: \quad \frac{d\bar{V}_x}{d\bar{y}} = 0, \quad \bar{\Omega} = 0; \\
\bar{y} = 0:
\end{aligned}$$

$$\begin{aligned} & \frac{\tau^+ \sigma_{yy}^+}{2} \frac{d\bar{V}_x}{d\bar{y}} - R^+ \left[V_y^+ + \frac{1 - k_n^2 k_t - (3/7) k_n (1 - k_t)}{1 + k_n (1 + k_t) + k_n^2 k_t} \left(\frac{2}{\pi} \sigma_{yy}^+ \right)^{1/2} \right] \times \\ & \quad \times \bar{V}_x = - \frac{2k_n R^+ \bar{\alpha}_2}{1 + k_n (1 + k_t) + k_n^2 k_t} \left(\frac{2}{\pi} \sigma_{yy}^+ \right)^{1/2} \bar{\Omega}, \\ \tau^+ \left(1 + \frac{\tau}{\tau_\omega} \right)^{-1} \sigma_{yy}^+ \frac{d\bar{\Omega}}{d\bar{y}} - R^+ \left[V_y^+ + \frac{1 - k_n^2 k_t + (3/7) k_n (1 - k_t)}{1 + k_n (1 + k_t) + k_n^2 k_t} \left(\frac{2}{\pi} \sigma_{yy}^+ \right)^{1/2} \right] \bar{\Omega} = \\ & \quad = - \frac{2k_n \bar{\beta}_1 R^+}{1 + k_n (1 + k_t) + k_n^2 k_t} \left(\frac{2}{\pi} \sigma_{yy}^+ \right)^{1/2} \bar{V}_x, \\ & \quad \bar{\alpha}_2 = \bar{d} (1 - k_t) / 7, \quad \bar{\beta}_1 = 10(1 - k_t) / (7\bar{d}), \quad \bar{d} = d_p / R. \end{aligned}$$

The intensity of the pulsating particle motion in the axial and normal directions is given by

$$\begin{aligned} & \frac{1}{(1 - \bar{y}) \bar{N}} \frac{d}{d\bar{y}} \left[(1 - \bar{y}) \bar{N} \frac{\tau^+ \sigma_{yy}^+}{3} \frac{d\sigma_{xx}^+}{d\bar{y}} \right] - R^+ V_y^+ \frac{d\sigma_{xx}^+}{d\bar{y}} - \frac{2R^{+2}}{\tau^+} \sigma_{xx}^+ = \\ & \quad = - \left[\frac{2R^{+2}}{\tau^+} \sigma_{xx}^+ + R^+ U_m^+ \text{St} \sigma_{yy}^+ \left(\frac{d\bar{V}_x}{d\bar{y}} \right)^2 \right], \\ & \quad \sigma_{xx}^+ = \frac{T^+}{\tau^+} e_{xx}^+ + \frac{\gamma_\omega^2}{2} \text{St} \frac{T^+ U_m^+}{R^+} e_{yy}^+ \bar{\Omega}^2 - \gamma_\omega \frac{\text{St}^2}{2} \sigma_{yy}^+ \bar{\Omega} \frac{d\bar{V}_x}{d\bar{y}}, \\ & \frac{1}{(1 - \bar{y}) \bar{N}} \frac{d}{d\bar{y}} \left[(1 - \bar{y}) \bar{N} \tau^+ \sigma_{yy}^+ \frac{d\sigma_{yy}^+}{d\bar{y}} \right] - R^+ V_y^+ \frac{d\sigma_{yy}^+}{d\bar{y}} - \frac{2R^{+2}}{\tau^+} \sigma_{yy}^+ = - \frac{2R^{+2}}{\tau^+} \sigma_{yy}^+, \\ & \quad \sigma_{yy}^+ = \frac{T^+}{\tau^+} e_{yy}^+ + \frac{\gamma_\omega^2}{2} \text{St} \frac{T^+ U_m^+}{R^+} e_{xx}^+ \bar{\Omega}^2 + \gamma_\omega \left(1 + \frac{\tau}{\tau_\omega} \right)^{-1} \text{St} (\bar{U}_x - \bar{V}_x) \sigma_{yy}^+ \frac{d\bar{\Omega}}{d\bar{y}} + \\ & \quad \quad + \frac{\gamma_\omega}{2} \text{St}^2 \sigma_{yy}^+ \bar{\Omega} \frac{d\bar{V}_x}{d\bar{y}}, \end{aligned} \tag{3.2}$$

in which $\sigma_{ij}^+ = \sigma_{ij} / u_+^2$; $e_{ij}^+ = \langle u_i u_j \rangle / u_+^2$; $T^+ = T_E u_+^2 / \nu$ is the dimensionless time scale of the turbulent gas pulsations. The boundary conditions for (3.2) are written from the symmetry condition at the axis and collision with the wall:

$$\begin{aligned} \bar{y} = 1: \quad & \frac{d\sigma_{xx}^+}{d\bar{y}} = \frac{d\sigma_{yy}^+}{d\bar{y}} = 0; \\ \bar{y} = 1: \quad & \tau^+ \sigma_{yy}^+ \frac{d\sigma_{yy}^+}{d\bar{y}} - R^+ \left[V_y^+ + 2 \frac{1 - k_n^3}{1 + k_n^3} \left(\frac{2}{\pi} \sigma_{yy}^+ \right)^{1/2} \right] \sigma_{yy}^+ = 0, \\ & \frac{\tau^+ \sigma_{yy}^+}{3} \frac{d\sigma_{xx}^+}{d\bar{y}} - R^+ \left[V_y^+ + \frac{1 - k_n \alpha_1^2}{1 + k_n \alpha_1^2} \left(\frac{2}{\pi} \sigma_{yy}^+ \right)^{1/2} \right] \sigma_{xx}^+ = 0. \end{aligned}$$

We incorporated the dependence of the relaxation times for the translational and rotational motion on the averaged relative velocity and rotational speed [1, 14]:

$$\begin{aligned} \tau &= \tau^0 (1 + \text{Re}_p / 60)^{-1}, \quad \tau^0 = (1/18) \rho_p / \rho_g d_p^2 / \nu, \\ \text{Re}_p &= |\bar{U}_x - \bar{V}_x| \bar{d} \text{Re} / 2, \quad \text{Re} = 2R U_m / \nu, \\ \tau_\omega &= \tau_\omega^0 (1 + \text{Re}_\omega^{1/2} / 7.8)^{-1}, \quad \tau_\omega^0 = (1/60) \rho_p / \rho_g d_p^2 / \nu, \\ & \quad \text{Re}_\omega = \bar{d}^2 \bar{\Omega} \text{Re} / 8. \end{aligned}$$

We estimated γ_ω from the [15] results: $\gamma_\omega = 6/\pi c_L \rho_g / \rho_p$, $c_L \approx 0.3$. The parameters of the carrying phase were calculated from a one-parameter turbulence model [16]. The intensity of the transverse gas velocity pulsations and the time scale of the energy-bearing pulsations are determined by the turbulence energy and the Nikuradze spatial scale L_E :

$$\langle u_y^2 \rangle = k_y E, \quad T_E = \gamma_E L_E / E^{1/2}, \quad k_y = 0.2, \quad \gamma_E = 1.16.$$

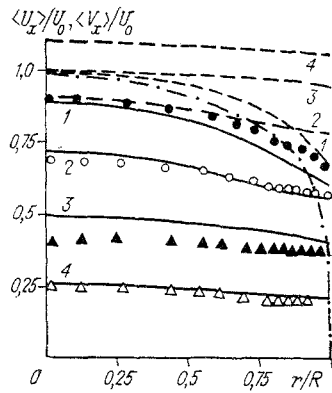


Fig. 1

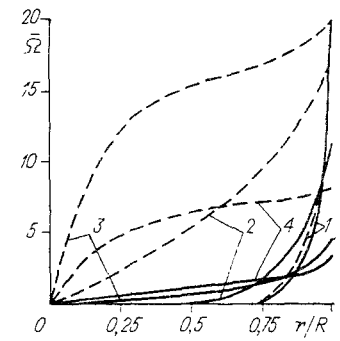


Fig. 2

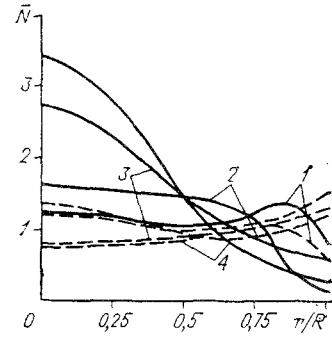


Fig. 3

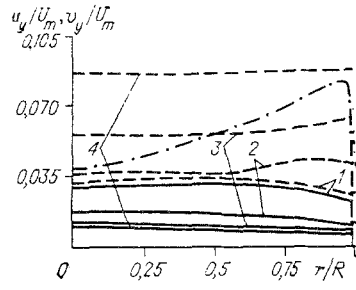


Fig. 4

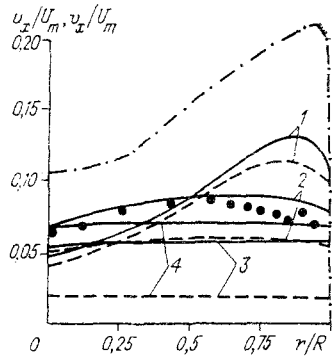


Fig. 5

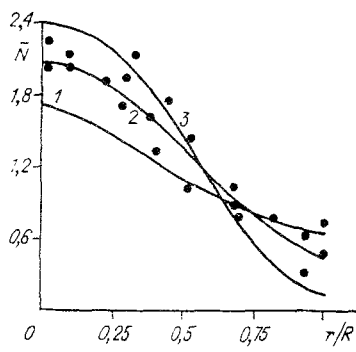


Fig. 6

Figures 1-5 show calculations on the powder in a vertical cylindrical channel with a rising flow (solid lines) or a descending one (dashed lines). The dot-dash lines show the characteristics of the carrying phase. The calculations are for the experimental conditions in [17]. Curves 1-4 correspond to particle diameters $d_p = 100, 200, 400, 800 \mu\text{m}$, and $k_n = k_t = 0.8$ (the experimental data are indicated by the points). There is a close correlation between the pulsating and averaged particle characteristics. Figure 1 shows the particle velocity distribution (U_0 is the gas velocity at the axis); the random motion transverse to the channel leads to rapid transport of the axial momentum component to the walls, and the momentum loss by collision causes considerable averaged phase velocity slip. The collisions give the particles rotation $\Omega_\theta > 0$ (Fig. 2). The maximum angular velocity is attained at the inner surface of the channel. The rotational velocities for small particles at the wall greatly exceed those of large ones, but because of the inertia, the angular velocities of the large particles fall less towards the center of the channel. In the flow region where the particles run ahead of the gas, the Magnus force is directed towards the surface, while where the particles lag behind the carrying phase, the Magnus force is directed towards the axis.

Figure 3 shows the particle concentrations in rising and descending flows. The concentration profile is affected by the turbulent migration, which is caused by the inhomogeneity in the pulsation pattern of the particle velocities normal to the surface and is directed to reducing the pulsating motion (Magnus force), while also being affected by turbulent diffusion, which reduces the concentration gradients. Figure 3 implies that the Magnus force plays an important part in producing the concentration profile for the larger particles in rising flow. The level of the turbulent velocity pulsations normal to the surface is less for the large particles than for the small ones (Fig. 4, $u_y = \langle u_y^2 \rangle^{1/2}$, $v_y = \langle v_y^2 \rangle^{1/2}$), while the turbulent migration velocity is small because of the homogeneous profile for the pulsation energy over the cross section. In the case of descending flow, the increase in the axial velocity of a particle at the wall causes an increase in the angular velocity by comparison with the lifting flow (Fig. 2), which in turn produces additional normal velocity pulsations for the powder (Fig. 4) and reduces the intensity of the axial velocity pulsations (Fig. 5, $u_x = \langle u_x^2 \rangle^{1/2}$, $v_x = \langle v_x^2 \rangle^{1/2}$ points for $d_p = 800 \mu\text{m}$). The increase in intensity of the random particle motion in the cross section is due to greater filling in the angular velocity profiles in descending flow (Fig. 2) and also the more uniform concentration profile (Fig. 3). The comparatively high level of pulsating motion for a large particle is obtained only when one incorporates the generation of random motion as a result of collisions with the walls.

Figure 6 compares calculations on the particle concentration ($d_p = 23 \mu\text{m}$) with experiment [18] for a high-velocity flow, when the effects of the gravitational force on the particle motion can be neglected (curves 1-3 correspond to velocities of $U_m = 98, 144, \text{m/sec}$). A bell-shaped concentration distribution in the channel can be obtained in the calculations only when one incorporates the Magnus force.

A statistical approach thus gives a closed description of the flow of a two-phase gas-solid suspensate in which the particles interact strongly with the channel walls.

LITERATURE CITED

1. A. A. Shraiber, L. B. Gavin, V. A. Naumov, and V. P. Yatsenko, *Turbulent Gas Suspensate Flows* [in Russian], Naukova Dumka, Kiev (1987).
2. S. Matsumoto, S. Saito, and S. Maeda, "Simulation of gas-solid two-phase flow in a horizontal pipe", *J. Chem. Eng. Japan*, 9, No. 10 (1976).
3. L. V. Kondrat'ev and V. V. Shor, "A study on the turbulent flow of a gas suspension in a tube with allowance for collisions with the wall and particle rotation", *Izv. AN SSSR, MZhG*, No. 1 (1990).
4. A. H. Govan, G. F. Hewitt, and C. F. Ngan, "Turbulent motion in a turbulent pipe flow", *Int. J. Multiphase Flow*, 15, No. 3 (1989).
5. J.-S. Shuen, L.-D. Chen, and G. M. Faeth, "Evaluation of a stochastic model of particle dispersion in a turbulent round jet", *AIChE J.*, 29, No. 1 (1983).
6. G. A. Kallio and M. W. Reeks, "A numerical simulation of particle deposition in turbulent boundary layers", *Int. J. Multiphase Flow*, 15, No. 3 (1989).
7. K. D. Squires and J. K. Eaton, "Particle response and turbulence modification in isotropic turbulence", *Phys. Fluids A: Fluid Dynamics*, 2, No. 7 (1990).
8. S. L. Lee, "Particle motion in a turbulent two-phase dilute suspension flow", *Particle and Particle Systems Characterization*, 6, No. 1 (1989).
9. I. V. Derevich and V. M. Eroshenko, "Calculation of the average velocity slip in turbulent flow of a two-phase mixture in a channel", *Izv. AN SSSR, MZhG*, No. 2 (1990).
10. I. N. Gusev and L. I. Zaichik, "Simulating particle dynamics in the wall region of a two-phase gas-particle turbulent flow", *Izv. AN SSSR, MZhG*, No. 1 (1991).
11. I. V. Derivich and V. M. Eroshenko, "Boundary conditions for the heat and mass transfer equations for coarse aerosols in turbulent flow", *Inzh.-Fiz. Zh.*, 61, No. 4 (1991).
12. V. I. Klyatskin, *Stochastic Equations and Waves in Randomly Inhomogeneous Media* [in Russian], Nauka, Moscow (1980).
13. K. Cherchin'yani, *Mathematical Methods in the Kinetic Theory of Gases* [Russian translation], Mir, Moscow (1973).
14. S. C. Dennis, S. N. Singh, and D. B. Ingham, "The steady flow due to a rotating sphere at low and moderate Reynolds numbers", *J. Fluid Mech.*, 101, No. 2 (1980).
15. Y. Tsuji, Y. Merikawa, and Y. Mizuno, "Experimental measurement of the Magnus force on a rotating sphere at low Reynolds numbers", *Trans. ASME, J. Fluids Eng.*, 107, No. 4 (1985).
16. I. V. Derevich, V. M. Eroshenko, and L. I. Zaichik, "Hydrodynamics and heat transfer of turbulent gas-suspension flows in tubes. 1. Hydrodynamics", *Int. J. Heat Mass Transfer*, 32, No. 12 (1989).

17. S. L. Lee and F. Durst, "On the motion of particles in turbulent duct flow", *Int. J. Multiphase Flow*, 1, No. 2 (1982).
18. B. A. Balanin and V. V. Zlobin, "An experimental study on the aerodynamic resistances of simple bodies in a two-phase flow", *Izv. AN SSSR, MZhG*, No. 3 (1979).

EFFECT OF FRACTURE RATE ON THE DYNAMICS OF THE INTERACTION
OF AN IMPACT LOAD PULSE WITH THE SURFACE OF A SOLID

A. V. Utkin

UDC 539.593

Studies of cleavage phenomena during the reflection of shock waves from the free surface of a body [1, 2] provide unique information about the strength properties of materials in the submicrosecond range. Under these conditions, however, the time to fracture is comparable with the loading time and as a result the experimental values of the cleavage strength of material, which is not a comprehensive characteristic, are not unique; it is thus necessary to speak of the breaking strength as a function of the strain rate as well as other state parameters. A number of papers (see, e.g., [3, 4]) have developed a semi-empirical continuum-kinetic model of fracture, which gives an acceptable description of particular cases when used in problems of mathematical simulation of shock-wave phenomena. At the same time, information must be obtained about the kinetic fracture laws directly from analysis of experimental data. Such information in implicit form is contained by the velocity profiles of the surface of the test specimen [5]. The fracture of the material after reflection of a shock wave from the free surface of a body and the attendant relaxation of tensile stresses give rise to a compression wave, a so-called cleavage pulse. Clearly, in the case of instantaneous fracture the cleavage pulse should have the steepest leading edge and the largest amplitude. It is intuitively clear that a longer time to fracture reduces the slope of the cleavage pulse. A prolonged decrease in velocity against the background of its damped oscillations has been also observed in experiments.

Our aim was to analyze wave processes in a fracturing medium upon reflection of a compression pulse from the free surface and to study the possibility of obtaining data on the fracture rate directly from measurements of the velocity profiles of the surface of the specimen.

Formulation and Solution of the Problem. In the acoustic approximation we consider the evolution of a triangular compression pulse after its reflection from the free surface of a specimen, which develops at negative pressure. We assume that fracture begins when the tensile stresses reach the critical value P_c and is characterized by a specific pore volume v_p . The total specific volume of the medium is equal to the sum of v_p and the specific volume of the solid component v_s : $v = v_p + v_s$. We use the simplest fracture kinetics: the rate of change of v_p depends linearly on the pressure P and is zero if $P > 0$ and $v_p = 0$. The system of hydrodynamic equations, closed by the kinetic equation and the equation of state, has the form (in Lagrange's variables)

$$\frac{\partial v}{\partial t} - \frac{1}{\rho_0} \frac{\partial u}{\partial h} = 0, \quad \frac{\partial u}{\partial t} + \frac{1}{\rho_0} \frac{\partial P}{\partial h} = 0, \quad \frac{\partial v_p}{\partial t} + \frac{P}{\rho_0^2 c_0^2 \tau_\mu} = 0, \quad P = \rho_0^2 c_0^2 (1/\rho_0 - v + v_p), \quad (1)$$

where t is the time; h is the Lagrange coordinate; u is the mass velocity; ρ_0 and c_0 are the initial density and the velocity of sound; and τ_μ is the characteristic relaxation time of the fracture process, corresponding to the bulk viscosity $\mu = \rho_0 c_0^2 \tau_\mu$. In the equation of state the pressure is determined from the solid component $v_s = v - v_p$.

Figure 1 shows the flow pattern in the t - h plane. In region 1 the incident wave and the reflected wave do not interact and the dependence of the mass velocity and pressure on the coordinates and time corresponds to a triangular compression pulse: